

## PRELIMINARY NUMERICAL AND EXPERIMENTAL TESTS FOR THE STUDY OF VIBRATION SIGNALS IN DRY GRANULAR FLOWS

FRANCESCO ZARATTINI<sup>1</sup>, ANTONIO POL<sup>1</sup>, LUCA SCHENATO<sup>2</sup>, PIA R. TECCA<sup>2</sup>, ANDREA M. DEGANUTTI<sup>2</sup>, ANDRÉS GARCIA-RUIZ<sup>4</sup>, MIGUEL SORIANO-AMAT<sup>4</sup>, MIGUEL GONZÁLEZ-HERRÁEZ<sup>4</sup>, HUGO F. MARTINS<sup>5</sup>, ALESSANDRO PASUTO<sup>2</sup>, LUCA PALMIERI<sup>3</sup>, FABIO GABRIELI<sup>1</sup>

<sup>1</sup> Department of Civil, Environmental and Architectural Engineering, University of Padova, Italy  
[francesco.zarattini@studenti.unipd.it](mailto:francesco.zarattini@studenti.unipd.it)

<sup>2</sup> Research institute for Geo-hydrological Protection, National Research Council, Padova, Italy

<sup>3</sup> Department of Information Engineering, University of Padova, Italy

<sup>4</sup> Department of Electronics, University of Alcalá, Madrid, Spain

<sup>5</sup> Instituto de Óptica, Consejo Superior de Investigaciones Científicas, Madrid, Spain

**Key words:** vibrations, debris flows, DEM, granular materials, distributed optical fiber sensing, distributed vibration sensing.

**Abstract.** Debris flows are one of the most important hazards in mountainous areas because of their paroxysmal nature, the high velocities, and energy carried by the transported material. The monitoring of these phenomena plays a relevant role in the prevention of the effects of these events. Among different possibilities, fiber optical sensors appear well-suited for this purpose thanks to their fair cheapness (with the exception of the interrogator), the robustness to electromagnetic interferences, the adaptability in extreme harsh conditions (no power supply is required), the possibility of locating the interrogator many kilometers far away from the monitored site, and the unique feature to provide very-dense multipoint distributed measurements along long distances. In this work, the vibro-acoustics signal produced by these phenomena has been focused as a possible source of information for the prediction of incipient movement, and the tracking of their path, velocity and thickness. Few literature works investigate these aspects, and for this reason, a preliminary laboratory and numerical campaign have been carried out with dry granular flume tests on an inclined chute. The discrete element method has been used to simulate the tests and to synthesize the signal measured on an instrumented mat along the channel. The grain shapes of the granular material used in simulations have been obtained by a photogrammetric tridimensional reconstruction. The force-time signal has been also analyzed in time-frequency domain in order to infer the features of the flow. The numerical activity has been preparatory for the experiments carried out by instrumenting the flume with an optical fiber distributed vibration sensing system.

## 1 INTRODUCTION

Debris flows are particularly hazardous slope instability phenomena due to the high speeds and high amount of energy that the transported material carries [1, 2]. Structures such as weirs and deposit areas are solutions that sometimes do not provide precautionary values of the safety factor. Therefore, monitoring plays a fundamental role in the prevention and mitigation of the effects produced by these flows. In addition to traditional methods (echometers, geophones, estensimeters), recent studies suggested the possibility of using distributed fiber optic sensors (DFOS) to monitor the flows [3, 4].

The DFOS technology employed in this study is the so-called distributed acoustic sensor (DAS), that is a promising sensing platform for many different applications in structural health monitoring, leak detection in pipelines, seismic wave detection, and many more geophysical applications.

With this technology, the fiber is probed by a coherent laser pulse and the DAS interrogator tracks the changes in the phase of the optical backscattered signal in time. The longitudinal strain exerted to the fiber is proportional to the recorded optical phase shifts between pulses and therefore, that shift can be mapped into the dynamic distributed strain field across a given fiber segment by integration.

In regard to the specific application addressed here by DAS technology, the optical fibre behaves as an equivalent array of many concatenated geophones (hundreds per kilometre of fibre length) capable of detecting acoustic perturbations and vibration in real time, over a frequency range up to a few kilohertz. As in other DFOS, the optical fibre acts here as both the communication channel and the sensing element. This unique feature of DOFS enables the reduction of the system complexity in particular for those applications requiring many hundreds of sensing points.

Furthermore, the DAS used in this study implements a novel interrogation scheme based on highly chirped probe pulses [5]. This technique is more robust than conventional DAS scheme, as it offers localised detection of the perturbation with the same spatial resolution and acoustic/vibration bandwidth of traditional implementation, where instead the perturbation effects cumulate along the fibre.

In this work, first step of a wider study, some tests on a channel with granular material were simulated using the discrete elements method (DEM). From the simulations the seismic signal produced by the passage of the material above a control plate placed on the bottom of the channel was obtained. Considering a priori significant the shape of the grains on the signal produced, this has been reproduced through rigid aggregates of spheres (clumps). The shape of an individual clump derives from a previous tridimensional scanning phase of some sample grains taken from the material used in the laboratory tests.

The goal of this study is to obtain preliminary information (numerically and experimentally) about the signal produced by a granular flow, in terms of vibrations, number of interactions, force and strain vs time and of their frequency content.

## 2 NUMERICAL SIMULATIONS

### 2.1 The geometry of the model

The simulated geometry is the same used in the subsequent laboratory tests but, in order to reduce the computational time and the amount of data storage (which has been collected for more than 350000 timesteps), the informations about the flow were collected only along one section along the channel, just above a measurement plate (Figure 1). The channel is 1.55 m long, 0.30 m large and inclined of  $38^\circ$  with respect to the horizontal plane. The measurement plate is 20 cm long and located 64.5 cm far away from the gate of the upper tank.

Initially the release mass is poured in the upper tank; then the lateral wall of the tank is removed and the granular material strats to flow. A larger box is used as deposit base as presented in Figure 1.

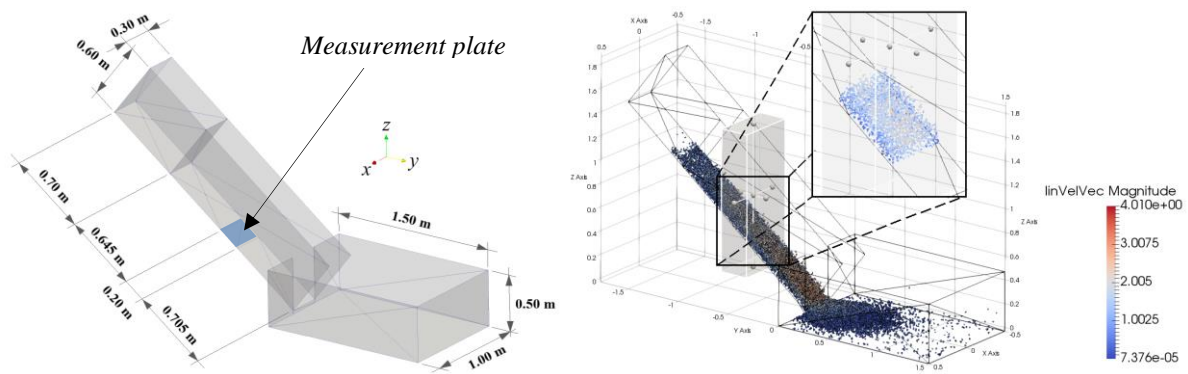


**Figure 1:** Geometry used for the numerical simulation of the dry granular flow.

A fixed granular volume of  $0.027 \text{ m}^3$  is used in each test; the initial porosity is 0.45 for  $\sim 40$  kg of mass. All simulations are performed using the open-source code Yade [6].

### 2.2 The granular material

Clumps of 4, 8, 16 spheres have been used in order to better mimic the real shape of the grains used in the experimental tests. For this purpose, 16 samples of grains were scanned through a stereo-photogrammetrical method based on the “Structure from motion” (SfM) ([7, 8]), the *Meshlab* software [9], and using a rotating platform.

The discretization of the mesh via polar spheres was performed with *Power Crust* [10] which implements the median axis approach. In Figure 2 an example of a reconstructed grain, discretized with a different number of spheres, is reported.

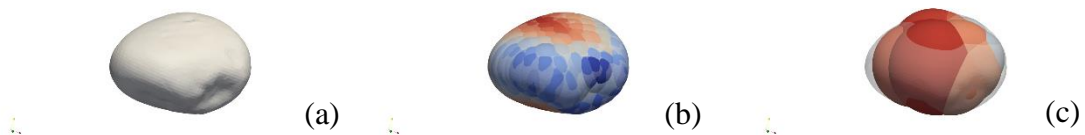


**Figure 1:** Example of clump generation: from (a) the surface mesh reconstruction, to a (b) 395 spheres and (c) 16 spheres representation.

The contact model was Hertz-Mindlin in normal direction, while the Mindlin theory was adopted in the tangential one [11]. The rolling and twisting resistance were neglected since their effect has been substituted by the better description of the grain shapes.

The Young modulus and the Poisson's ratio at the contact were set  $E=10^8$  Pa,  $\nu=0.2$  for both the clumps and the walls. The contact friction angle was  $40^\circ$  while the normal and tangential restitution coefficient of the contact sphere-sphere and wall-sphere were 0.8 and 0.4 respectively.

### 2.3 Numerical results

The registration of the data started at time  $t_0$  when one particle crossed the control volume above the measurement plate.

After that, at each time step, impact force components along the three axes have been recorded, as well as the number of clump-plate interactions. Moreover, every 0.025 s the coordinates of the centers of each sphere in the volume above the plate, and their linear ( $v_x, v_y, v_z$ ) and angular velocities ( $\omega_x, \omega_y, \omega_z$ ), have been stored.

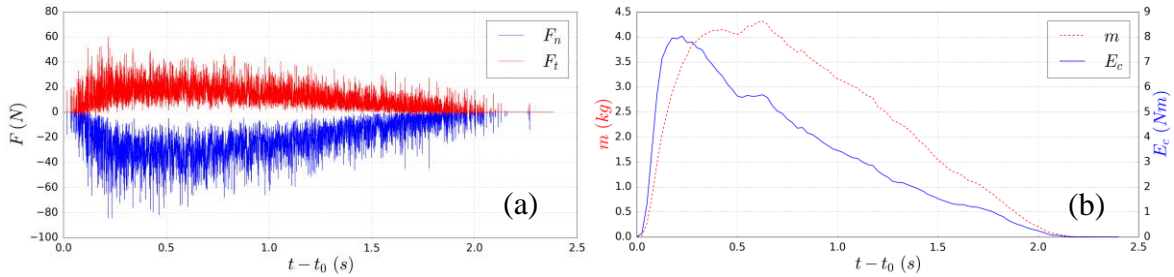


**Figure 3:** (a) Trends of normal and tangential forces and (b) of the mass and translational kinetic energy above the measurement plate.

From the collected data it is possible to obtain the seismic signal transmitted from the dry granular flow, its spectrogram, together with kinetic energies obtained from the velocities.

For the sake of brevity we refer here only to the results of the simulation obtained with the smooth pebbles of 11.2-16 mm diameter, and represented with 16 spheres per clump.

The trend of the normal force  $F_n$  and the tangential force  $F_t$  with the time is reported in Figure 3(a), while the mass and the translational kinetic energy on the control volume above the plate, are showed in Figure 3(b).

The high variability of the force signals is due to the continuous creations and destructions of contact force chains [12] between the particles and the measurement plate. The mean force signal presents a peak at 0.5 seconds while the peak of kinetic energy precedes the peak of mass: it occurs at  $t - t_0 = 0.25$  s and in correspondence of the maximum variability of the forces.

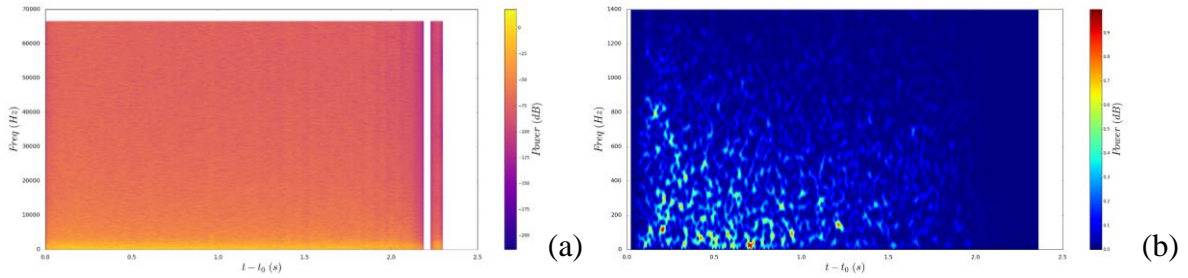


**Figure 4:** (a) Spectrogram obtained from the normal impact forces  $F_n$  and (b) PSD spectrogram of the same force, limited to the frequency of 1.4 kHz.

In Figure 4(a) and (b) the spectrograms of the signal generated by  $F_n$  are reported. The maximum frequency detected is almost 70 kHz. But, if a narrower frequency range is investigated (up to 1.4 kHz), it can be observed that the higher power of the signal is concentrated within this range (see Figure 4(b)). These numerical results have been used to set the spatial and temporal resolution of the DAS system used in the experimental tests.

### 3 EXPERIMENTAL TESTS

The laboratory setup consists of a chute of the same dimensions of the one used for the numerical simulations (the geometry is reported in §2.1). An engineered mat, embedding the optical fiber, has been opportunely designed and placed at the bottom of the flume: the mat is constituted by high-density polyethylene foam and embeds 20 PVC mandrels (diameter 5 cm, height 2 cm) – each coiled with approximately 40 m of optical fiber and the surface of the mat, exposed to the debris, is protected by a 3 mm rubber sheet. Overall, approximately 800 m of fiber are embedded in the mat.

The 20 mandrels are arranged in two sets of 10, at the right and left side of the flume, at 8 cm from the lateral walls. Along the flume, from bottom to the top, the coils of the two sets are at 15, 27.5, 40, 57.5, 75, 91.6, 108.2, 125, 145 and 165 cm.

Having a spatial sampling of 2 meters, 20 sampling points per each coils are measured. Please note that the DAS spatial resolution is 4 m, and correspondingly, each coil corresponds to an equivalent array of 10 geophones, while the signals collected in the entire mat correspond to an equivalent array of 200 geophones. The signal collected by the DAS, is expressed as the variation of axial strain inside the optical fiber with respect to the time, given the sampling frequency  $f_s$  of 1 kHz. The amount of data collected per each experiments is very huge and it is still under analysis: here, some preliminary results will be presented, mainly to show the feasibility of the approach and the great potential of the DAS technology.

For example, Figure 5 shows the signals collected at the coil on the right side, 75 cm from the bottom of the flume, during the flow test with sharp-edges grains of dimensions 11.2-16 mm. Such coil is situated approximately in the same position of the measurement plate in the numerical simulations.

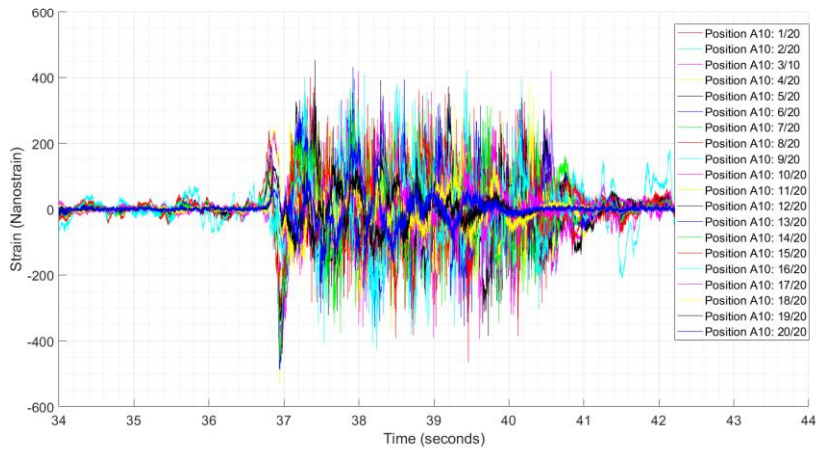


**Figure 5:** Strain in the 20 sampling points of one coil during the test with angular grains and grain size 11.2-16mm.

In order to measure the velocity of the flow, the energy carried by the signal has been considered. The energy of the debris obtained from a coil has been considered as the average of the energies detected by every single sampling point.

In Figure 6 the mean energy of the debris in correspondence of each coil with respect to the time is reported. By analyzing its evolution, it is possible to identify the instant at which the front of the flow reaches each coil: the black spots in Figure 6(b) report the instants in which the energy of the signal is considered to be representative of the front of the flow of the material. Finally, in Figure 7 the instants in which every coil is reached by the front of the flow are reported. The data shows a position-time trend, with a quite constant front velocity in the considered section.

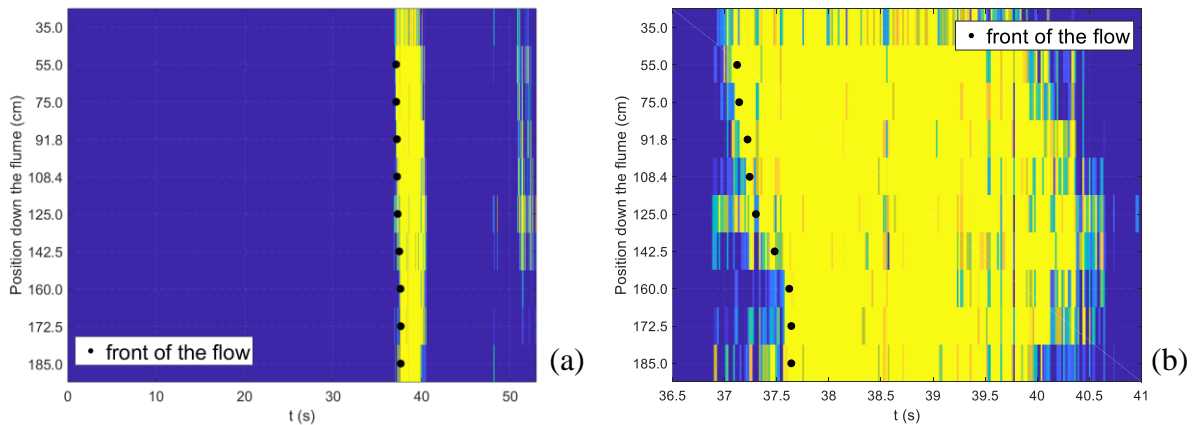


**Figure 6:** Mean energy measured by each coil on the right side along the chute with respect to the whole acquisition time, (b) with respect to the flow event.

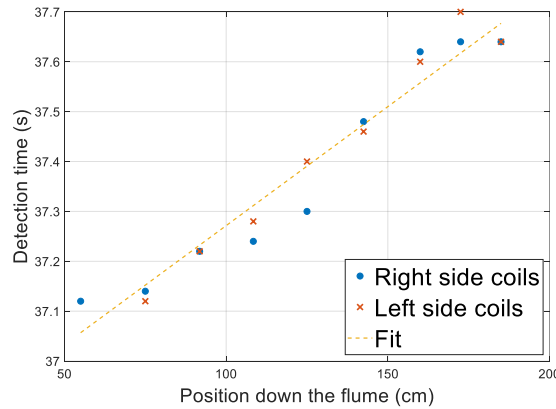


**Figure 7:** Instants in which the front reaches the left and the right sides coils along the flume.

## 4 CONCLUSIONS

From the preliminary numerical results highlighted in this work, it was shown that the signal generated by a granular flow is given by two contributions: one is related to the mass of the flow and one is related to its kinetic energy. The two contributions do not present simultaneous peaks in a given section: in our test, the first is the peak of kinetic energy which corresponds to the peak of force fluctuation. The peak of the mass instead is related to the thickness of the flow and it arrives after the front.

Moreover, observing the spectrograms, two different behaviours in terms of power emitted at different frequencies can be seen: a high power concentrated within a narrow frequency range; a low power spread in a wide frequency range. This means that the seismic signal is given by a sum of a low frequency signal – due to the mass of the material, that can be expressed as the thickness of the flow on the recording plate – and a high frequency signal, which is generated by the collisions. This preliminary analysis made it possible to reconstruct, although in a simplified manner, the signal produced by a granular flow.

This information has been used for the parameters used in the fiber optic measurement tool, based on Distributed Acoustic Sensing technology.

By the analysis of the signal recorded by the DAS, some preliminary results were obtained: in particular, evaluating the mean debris energy on each coil, it was possible to detect the kinematic of the front flow.

## ACKNOWLEDGEMENTS

This work is partly funded through the contribution of the DOMINO JPI WaterWorks project.

## REFERENCES

- [1] Iverson, R., Reid, M. & LaHusen, R. (1997), Debris-flow mobilization from landslides.

- Earth and Planetary Science Letters, 85-138.
- [2] Iverson, R. (1997), The Physics of Debris Flow. *Reviews of Geophysics*, 245–296.
  - [3] Michlmayr, G.; Chalari, A.; Clarke, A.; Or, D. Fiber-optic high-resolution acoustic emission (AE) monitoring of slope failure. *Landslides* 2017, 14, 1139–1146.
  - [4] Schenato, L. A Review of Distributed Fibre Optic Sensors for Geo-Hydrological Applications. *Appl. Sci.* 2017, 7, 896.
  - [5] J. Pastor-Graells, H. F. Martins, A. Garcia-Ruiz, S. Martin-Lopez, and M. Gonzalez-Herraez, "Single-shot distributed temperature and strain tracking using direct detection phase-sensitive OTDR with chirped pulses," *Opt. Express* 24, 13121-13133 (2016)
  - [6] Šmilauer, V. et al. (2015), Yade Documentation 2nd ed. The Yade Project. DOI 10.5281/zenodo.34073 (<http://yade-dem.org/doc/>).
  - [7] Wu, C., Agarwal, S., Curless, B. and Seitz, S. M. (2011), Multicore Bundle Adjustment, CVPR.
  - [8] Wu, C. (2013), Towards Linear-time Incremental Structure From Motion, 3DV.
  - [9] Ranzuglia, G., Callieri, M., Dellepiane, M., Cignoni, P., Scopigno, R. (2013), MeshLab as a complete tool for the integration of photos and color with high resolution 3D geometry data, *CAA 2012 Conference Proceedings*, page 406-416.
  - [10] Amenta, N., Choi, S., Kolluri, R. K., The Power Crust, University of Texas at Austin.
  - [11] Johnson, K. L., Contact mechanics, *Cambridge University Press, Cambridge, UK*, 1985.
  - [12] Lingran, Z., Nho Gia Hien Nguyen, Lambert S., Nicot F., Prunier F. & Djeran-Maigre I. (2016), The role of force chains in granular materials: from statics to dynamics, *European Journal of Environmental and Civil Engineering*, DOI.